

## Formation of ZnS/SiO<sub>2</sub> nanocables

Xia Fan,<sup>a)</sup> Xiang-Min Meng,<sup>b)</sup> Xiao-Hong Zhang,<sup>c)</sup> and Shi-Kang Wu

*Nano-Organic Photoelectronic Laboratory, Technical Institute of Physics and Chemistry, Chinese Academy of Sciences, Beijing 100101, People's Republic of China*

Shuit-Tong Lee

*Nano-Organic Photoelectronic Laboratory, Technical Institute of Physics and Chemistry, Chinese Academy of Sciences, People's Republic of China and Center of Super-Diamond and Advanced Films and Department of Physics and Materials Science, City University of Hong Kong, Hong Kong SAR, People's Republic of China*

(Received 3 December 2004; accepted 9 March 2005; published online 21 April 2005)

Nanometer-sized coaxial cables with a single-crystal ZnS core and a thin amorphous SiO<sub>2</sub> shell were synthesized by simple thermal evaporation in vacuum. As-fabricated ZnS/SiO<sub>2</sub> nanocables were studied using scanning electron microscopy, x-ray diffraction and transmission electron microscopy. The ZnS/SiO<sub>2</sub> nanocables have diameters of  $\sim 50$  nm, lengths of several tens of micrometers, and shell thickness of  $\sim 4$  nm. The core of the nanocable has a wurtzite structure with a growth direction along [001]. The nanocables show strong photoluminescence with two peaks related to band gap and defect-related emission. © 2005 American Institute of Physics. [DOI: 10.1063/1.1919394]

Nanosized semiconductor structures have been investigated extensively during the last decade for their optical and electronic properties, which are often different from the corresponding bulk materials. When their size is smaller than the Bohr exciton radius, the nanostructures exhibit evident quantum confinement and nonlinear optical behavior.<sup>1,2</sup> ZnS is an important group II–VI semiconductor, with a band gap of  $\sim 3.6$  eV at room temperature, and have been used in photonics research, electroluminescent devices, solar cells, and laser, etc.<sup>3–5</sup> It has also been used for mechano-optic applications, because ZnS doped with select metallic ions is a promising material which emits intense light upon stressing.<sup>6</sup> One-dimensional (1D) ZnS structures have recently attracted much attention due to their unique optical properties. A variety of 1D forms of ZnS material, including ZnS nanowires (or nanorods),<sup>7–11</sup> nanoribbons (or nanobelts),<sup>12,13</sup> nanotubes,<sup>14</sup> and bicrystal nanoribbons,<sup>15</sup> have been synthesized by simple methods based on thermal evaporation.

High chemical reactivity is often observed in some nanoscaled materials due to their high surface-to-volume ratio. The chemical reactivity can lead to oxidation and contamination of nanowires, resulting in dramatic changes in structure, morphology, and properties.<sup>16</sup> In our previous studies, we found that ZnS nanowires could be easily damaged by electron beam irradiation.<sup>10–12</sup> From the application viewpoint, it is important to suppress surface chemical reactivity. One possible solution is to wrap the nanomaterials with a dense and stable protective shell. Recently, ZnS/Si side-by-side biaxial nanowires<sup>17</sup> have been successfully obtained, which prevent surface oxidation of the ZnS nanowires to some degree. In this letter, we report the synthesis of ZnS nanowires wrapped inside a thin layer of SiO<sub>2</sub> for protection against oxidation and electron irradiation.

The synthesis of ZnS/SiO<sub>2</sub> nanocables was carried out in a high temperature and high vacuum tube furnace. An alumina tube was mounted inside the tube furnace and used as the reaction chamber. SiO powder was loaded into a ceramic boat placed at the center area of the tube, and ZnS powder was placed at a location 10 cm downstream of the SiO source. Si wafers were placed further downstream from the ZnS powder. The tube was sealed and evacuated to a pressure of  $2 \times 10^{-5}$  Torr. High-purity Ar was then fed at 50 sccm from one end of the tube toward the other where the silicon wafers were located. The furnace was then heated up from room temperature at a rate of 10 °C/min. When the temperature reached 1100 °C, the temperature was maintained for another 4 h before the furnace was cooled down naturally. During the whole process, the Ar flow was maintained and the pressure was kept at 10 Torr. After the furnace was cooled to room temperature, white wool-like products collected from the Si wafers were characterized using x-ray diffraction (XRD) with Cu K $\alpha$  radiation (Siemens D-500), scanning electron microscopy (SEM; Hitachi S-4300FEG), transmission electron microscopy (TEM; Philips CM20 and CM200 FEG) with energy-dispersive x-ray spectrometry (EDS). Photoluminescence (PL) of the as-grown ZnS/SiO<sub>2</sub> nanocables was measured at room temperature in a spectral range of 320–580 nm using a Ti:sapphire laser line of 300 nm as the excitation source.

For SEM investigations, the processed Si wafers were directly loaded into the SEM, without disturbing the original nature of the deposition products. Figure 1(a) shows that the deposition product consists of a high density of partially oriented nanowires with lengths up to several micrometers. A high-magnification SEM image [Fig. 1(b)] shows that most of the nanowires have uniform diameters in the range of 20–50 nm. Metallic particles were observed neither at the tip nor on the body of the nanowires.

A powder XRD spectrum of the nanowires is shown in Fig. 2. The diffraction peaks can be indexed as (100), (002), (101), (102), (110), (103), and (112) of the wurtzite-structured (hexagonal) ZnS phase with lattice constants of  $a=3.81$  Å and  $c=6.24$  Å (JCPDS file: 36-1450;  $a$

<sup>a)</sup>Also at: Graduate School of Chinese Academy of Sciences, Beijing, P. R. China.

<sup>b)</sup>Author to whom correspondence should be addressed; electronic mail: xmmeng@mail.ipc.ac.cn

<sup>c)</sup>Author to whom correspondence should be addressed; electronic mail: xhzhang@mail.ipc.ac.cn

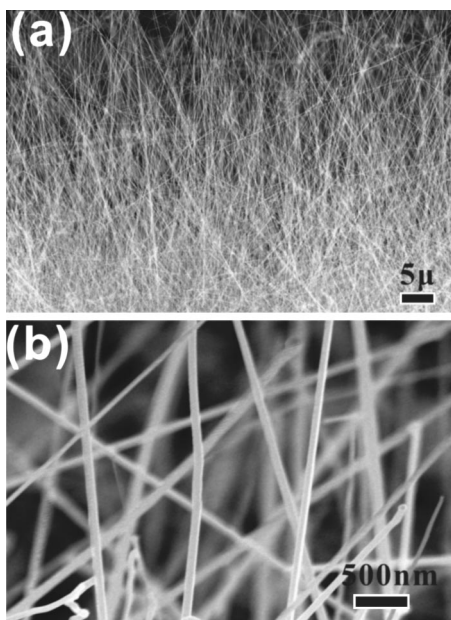


FIG. 1. (a) Low-magnification SEM image showing a high density of ZnS/SiO<sub>2</sub> nanocables over a large area; (b) an enlarged SEM image of the deposited nanocables.

$a=3.8298 \text{ \AA}$  and  $c=6.2573 \text{ \AA}$ ). No characteristic peaks due to impurities, such as Zn and ZnO, were detected. The relative intensities of different peaks in the spectrum of the nanowires differ considerably from those in the JCPDS file. In particular, the nanowire sample has a strong (002) peak while the (100) peak is the strongest in the JCPDS pattern. As the ZnS nanowires have a tendency to lie along their length (or on their widest facets) when they are dispersed on a glass sample holder, the x-ray data suggest that the nanowires have a preferential orientation of [001].

Detailed structure and composition of the products were characterized using TEM, EDS, and selected area electron diffraction (SAED). Figure 3(a) shows a low-magnification TEM image of the as-grown ZnS nanowires. It confirms that most wires have a uniform diameter of  $\sim 50 \text{ nm}$ , while a small part of them have uniform diameters of 60–70 and 20–30 nm. Figure 3(b) is a low-magnification high-resolution TEM image of a typical ZnS nanowire. A thin shell of about 4 nm thick with a lighter contrast can be clearly observed along the length of the nanowire. Figure 3(c) shows the EDS spectrum of the nanowires, which reveals the presence of Zn, S, Si, and O (also Cu signal comes

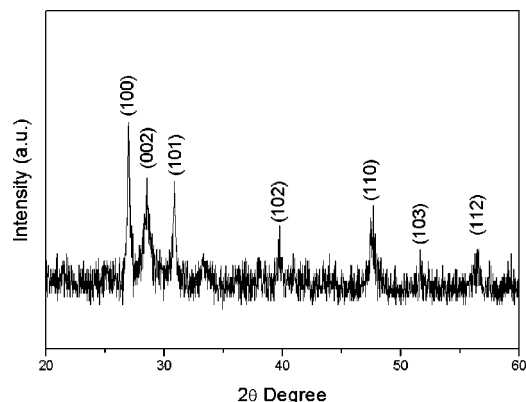


FIG. 2. XRD spectrum of ZnS nanocables.

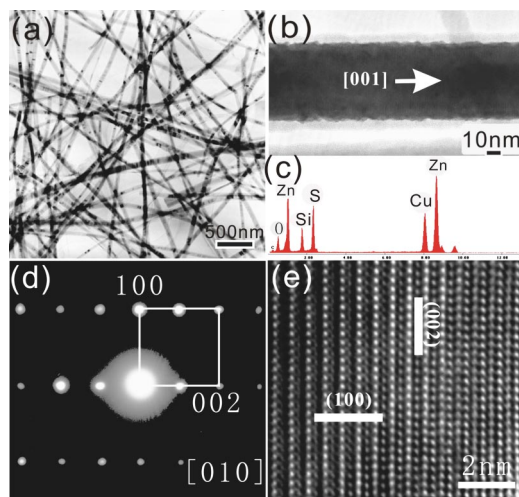


FIG. 3. (a) Low-magnification bright-field TEM image of ZnS nanocables; (b) A low-magnification high resolution TEM image of a nanocable; (c) An energy-dispersive spectrum; (d) A selected area electron diffraction pattern; and (e) An enlarged high resolution TEM image of the cable in (b).

from the Cu TEM sample grid). The atomic ratios of Zn–S and Si–O are close to 1:1 and 1:2, respectively. Figure 3(d) shows a typical SAED pattern of the nanowire. It can be indexed as the [010] zone axis diffraction pattern of the wurtzite ZnS single crystal. These results confirm that the wire is in fact a coaxial cable with a single crystalline ZnS core and an amorphous SiO<sub>2</sub> sheath.

Figure 3(e) is an enlarged high resolution TEM image of the nanocable in Fig. 3(b). The lattice fringes of (100) and (001) planes with the  $d$  spacings of  $\sim 0.38 \text{ nm}$  and  $\sim 0.63 \text{ nm}$  of the wurtzite ZnS can be clearly seen. This image shows that the cable is grown in [001] direction (or the  $c$  axes which is also the closest stacking direction). Neither dislocation nor stacking fault was observed. Unlike the case of bare ZnS nanowires,<sup>10</sup> the nanocables are stable under electron bombardment and show no observable changes after minutes of irradiation with 200 keV electrons. Such TEM examination has been repeated for several tens of individual nanocables and the above observations are representative.

Figure 4 shows the room-temperature PL spectrum of the ZnS nanocables. The spectrum has two peaks centered at  $\sim 334$  and  $\sim 520 \text{ nm}$ . The band at  $\sim 334 \text{ nm}$  corresponds to the band-gap emission of 3.70–3.49 eV, which is similar to that observed in ZnS nanowires.<sup>10</sup> The green emission at 520 nm may be caused by the presence of ZnS self-activated luminescence centers, probably arising from the vacancy states and interstitial states, or oxygen deficiency of SiO<sub>2</sub> sheath<sup>18</sup> to the peculiar nanostructures.

The growth of the ZnS/SiO<sub>2</sub> nanocables discussed above was accomplished by simple thermal evaporation of ZnS and

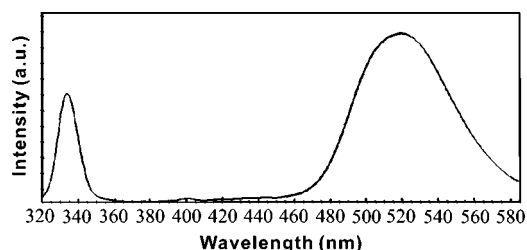


FIG. 4. PL spectrum of ZnS nanocables.

SiO powders. The growth is proposed to proceed as follows. The ZnS powders would first evaporate to produce ZnS vapor. The as-formed ZnS vapor would then be carried by the processing gas (Ar flow at a rate of 50 sccm) and travel to the lower temperature regions in the furnace tube, where it would deposit as ZnS nanoparticles (or nanoclusters) *via* homogeneous nucleation. The ZnS nanoparticles (or nanoclusters) are energetically favorable and serve as the stable sites for rapid adsorption of additional ZnS molecules, resulting in the formation of ZnS nanowires. In the present case, as no evidence for catalyst particles was observed on any tips of the synthesized nanowires, therefore the vapor–solid (VS) mechanism would be a reasonable explanation for the growth of the ZnS nanowires. With further increase of processing temperature, evaporation of SiO powders led to the formation of SiO<sub>x</sub> vapors.<sup>19</sup> Upon condensation and subsequent disproportionation of the SiO<sub>x</sub> vapor, a thin layer of Si and SiO<sub>2</sub> would grow on the as-grown ZnS nanowires, leading to the formation of ZnS/(Si+SiO<sub>2</sub>) core-shell nanocables. In our synthesis chamber, due to the residual sources of oxygen, such as the low content of H<sub>2</sub>O (~20 ppm) and oxygen in air adsorbed on the Si wafers, the thin Si layers on the ZnS nanowires would be *in situ* oxidized to form SiO<sub>2</sub>, finally resulting in the transformation of ZnS/(Si+SiO<sub>2</sub>) nanocables to ZnS/SiO<sub>2</sub> nanocables. Therefore, the present growth process is similar to the synthesis of Si crystalline tubular nanostructures using ZnS nanowires as templates *via* the evaporation method,<sup>14</sup> except that in our case the Si thin layers (or SiO<sub>2</sub> thin layers) are the constituent of the final ZnS/Si nanocables (or ZnS/SiO<sub>2</sub> nanocables). The detailed growth mechanisms of the nanostructures, however, are not fully understood.

The present ZnS/SiO<sub>2</sub> nanostructures are expected to possess the following unique features: (i) The combination of the insulating properties of the SiO<sub>2</sub> thin shell and excellent optical properties of the ZnS core would constitute a natural optical waveguide nanocable; and (ii) the creation of the chemically inert SiO<sub>2</sub> shell around the ZnS core could be an effective approach to prevent oxidation of ZnS nanowires (little oxidation was detected even after the samples were exposed to air for several months); (iii) SiO<sub>2</sub> sheath can prevent the damage of ZnS nanowires under electron beam or ion beam irradiation. It is expected that the present growth

method should be widely applicable for preparing a protective oxide surface on other nanosized materials.

In summary, coaxial nanocables composed of a single-crystal ZnS core and an amorphous SiO<sub>2</sub> shell have been fabricated by simple thermal evaporation of ZnS and SiO powders. The nanocables have diameters of ~50 nm, lengths of several tens micrometers, and shell thickness of 4 nm. The nanocable core has a wurtzite structure and growth direction of [001].

This work is supported by the Chinese Academy of Sciences, China and CAS-Croucher Joint Laboratory. STL thanks the support (Project no: CityU 2/02C) of the Research Grants Council of Hong Kong SAR, China.

<sup>1</sup>L. E. Brus, *J. Phys. Chem.* **90**, 2555 (1990).

<sup>2</sup>Y. Wang and N. Herron, *J. Phys. Chem.* **95**, 525 (1991).

<sup>3</sup>S. Kishimoto, A. Kato, A. Naito, Y. Sakamoto, and S. Iida, *Phys. Status Solidi C* **1**, 391 (2002).

<sup>4</sup>X. Jiang, Y. Xie, J. Lu, L. Zhu, W. He, and Y. Qian, *Chem. Mater.* **13**, 1213 (2001).

<sup>5</sup>T. V. Prevenslik, *J. Lumin.* **87**, 1210 (2000).

<sup>6</sup>M. F. Bulanyi, A. V. Kovalenko, and B. A. Polezhaev, *Inorg. Mater.* **39**, 222 (2003).

<sup>7</sup>C. S. Yang, D. D. Awschalom, and G. D. Stucky, *Chem. Mater.* **14**, 1277 (2002).

<sup>8</sup>Y. W. Wang, G. W. Meng, L. D. Zhang, C. H. Liang, J. Zhang, *Chem. Mater.* **14**, 1773 (2002).

<sup>9</sup>C. Ma, D. Moore, J. Li, and Z. L. Wang, *Adv. Mater. (Weinheim, Ger.)* **15**, 228 (2003).

<sup>10</sup>X. M. Meng, J. Liu, Y. Jiang, W. W. Chen, C. S. Lee, and S. T. Lee, *Chem. Phys. Lett.* **382**, 434 (2003).

<sup>11</sup>Y. Jiang, X. M. Meng, J. Liu, Z. R. Hong, C. S. Lee, and S. T. Lee, *Adv. Mater. (Weinheim, Ger.)* **15**, 1195 (2003).

<sup>12</sup>Y. Jiang, X. M. Meng, J. Liu, Z. Y. Xie, C. S. Lee, and S. T. Lee, *Adv. Mater. (Weinheim, Ger.)* **15**, 323 (2003).

<sup>13</sup>Q. Li and C. R. Wang, *Appl. Phys. Lett.* **83**, 359 (2003).

<sup>14</sup>J. Q. Hu, Y. Bando, J. H. Zhan, and D. Golberg, *Angew. Chem., Int. Ed.* **43**, 4606 (2004).

<sup>15</sup>X. M. Meng, Y. Jiang, J. Liu, C. S. Lee, and S. T. Lee, *Appl. Phys. Lett.* **83**, 2244 (2003).

<sup>16</sup>Y. C. Zhu, Y. Bando, D. F. Xue, and F. F. Xu, and D. Golberg, *J. Am. Chem. Soc.* **125**, 14226 (2003).

<sup>17</sup>J. Q. Hu, Y. Bando, Z. W. Liu, T. Sekiguchi, D. Golberg, and J. H. Zhan, *J. Am. Chem. Soc.* **125**, 11306 (2003).

<sup>18</sup>M. Zhang, E. Ciocan, Y. Bando, K. Wada, L. L. Cheng, and P. Pirouz, *Appl. Phys. Lett.* **80**, 491 (2002).

<sup>19</sup>W. S. Shi, H. Y. Peng, L. Xu, N. Wang, Y. H. Tang, and S. T. Lee, *Adv. Mater. (Weinheim, Ger.)* **12**, 1927 (2000).

Applied Physics Letters is copyrighted by the American Institute of Physics (AIP).  
Redistribution of journal material is subject to the AIP online journal license and/or AIP  
copyright. For more information, see <http://ojps.aip.org/aplo/aplcr.jsp>